Event-Triggered Multi-Lane Fusion Control for 2-D Vehicle Platoon Systems with Distance Constraints

Zepeng Zhou, Fanglai Zhu, Dezhi Xu, *Senior Member, IEEE*,
Boli Chen, *Member, IEEE*, Shenghui Guo, and Yuchen Dai

***Abstract*—This paper investigates the event-triggered fixed-time multi-lane fusion control for vehicle platoon systems with distance keeping constraints where the vehicles are spread in multiple lanes. To realize the fusion of vehicles in different lanes, the vehicle platoon systems are firstly constructed with respect to a two-dimensional (2-D) plane. In case of the collision and loss of effective communication, the distance constraints for each vehicle are guaranteed by a barrier function-based control strategy. In contrast to the existing results regarding the command filter techniques, the proposed distance keeping controller can constrain the distance tracking error directly and the error generated by the command filter is coped with by adaptive fuzzy control technique. Moreover, to offset the impacts of the unknown system dynamics and the external disturbances, an unknown input reconstruction method with asymptotic convergence is developed by utilizing the interval observer technique. Finally, two relative threshold triggering mechanisms are utilized in the proposed fixed-time multi-lane fusion controller design so as to reduce the communication burden. The corresponding simulation results also verify the effectiveness of the proposed strategy.**

***Index Terms*—multi-lane fusion, distance constraints, unknown input reconstruction, fixed-time control, event-triggered control**

I. Introduction

DUE to the technological development of the Internet of things devices, the issues regarding the intelligent traffic control have been discussed frequently [1]. Among these, many significant vehicle platoon control strategies have been designed with guaranteed string stability [2]. Retrospecting the existing researches, the vehicle platoon control strategies can be categorized into two main classes, namely the adaptive cruise control (ACC) and the cooperative adaptive cruise control (CACC) [3]. For the ACC control strategy, one of the main targets is keeping a safe following between each two consecutive vehicles. Based on this demand, the control input of the ACC is usually constructed by the signals obtained from automotive radars. However, when the platoon systems are confronted with a complicated environment or the vehicles move at high speeds, the reliability of the ACC is questionable. As an alternative, the CACC technique has been investigated extensively. One of the major differences between the CACC and the ACC approaches is that the CACC enables vehicles in the platoon to share control and state information with the help of wireless communication techniques [4]. Nevertheless, it should be noted that most of the existing results about the CACC and the ACC mainly focus on the string stability analysis for one dimensional (1-D) scenarios. This restricts the real application of these control strategies. As an extension, some remarkable researches have been done even for two dimensional (2-D) plane. In [5], the so-called openCDA simulation platform is constructed and a convenient way to deploy CACC algorithm is provided. In [6], the multi-lane fusion decision in 2-D plane is discussed from strategic and tactical level. In the present paper, the string stability of the vehicle platoon is analyzed within 2-D plane under the CACC control framework and the multi-lane fusion control schemes for vehicles spread in different lanes are proposed as well.

Although many researches have be conducted on the string stability issues of the vehicle platoon, the time-varying constraints on the distance tracking errors are seldom considered in literature [7]. During the vehicle moving process, two main problems must be solved properly, namely, the vehicle collision avoidance and the limitations on vehicle communication range [8]. One promising approach for addressing these problems is output constraint control strategies which involve the prescribed performance control, barrier Lyapunov function and funnel control [9]. By importing the given performance function, the controller in [7] is able to prevent connectivity breaks and collisions. By integrating a terminal sliding mode surface and a barrier Lyapunov function, the distance keeping is ensured in [10] even under an actuator faulty scenario. In [11], the collision avoidance integrating with the effective communication range is considered when constructing a $\arctan$-function-based prescribed performance controller. In [12], the desired distance is ensured by a $\log$-function for a 2-D vehicle platoon while the time-varying tracking error boundaries are considered. By integrating the barrier function notion, the prescribed performance controller with $\arctan$-function in [13] can guarantee the desired distance gap for the 2-D vehicle. In [14], the collision avoidance constraint is interpreted as a transformation error and a safe distance is maintained by stabilizing the transformation error. Moreover, to offset the external disturbance accurately, a sliding mode

Manuscript received XXX; revised XXX. This work was supported by National Natural Science Foundation of China under Grant No. 61973236, 61573256 and 61973140. (Corresponding author: Fanglai Zhu)

Zepeng Zhou and Fanglai Zhu are with the College of Electronics and Information Engineering, Tongji University, Shanghai, 201804, China. (e-mail: chowzepeng@tongji.edu.cn, zhufanglai@tongji.edu.cn)

Dezhi Xu is with the School of Internet of Things Engineering, Jiangnan University, Wuxi, 214122, China. (e-mail: xudezhi@jiangnan.edu.cn)

Boli Chen is with the Department of Electronic and Electrical Engineering, University College London, London WC1E 6BT, U.K. (e-mail: boli.chen@ucl.ac.uk)

Shenghui Guo is with the College of Electronics and Information Engineering, Suzhou University of Science and Technology, Suzhou, 215009, China. (email: shguo@usts.edu.cn)

Yuchen Dai is with the School of Automation, Wuhan University of Technology, Wuhan 430070, China. (e-mail: whutdyc@126.com)

disturbance observer is imported in the platoon controller in [15]. Retrospecting these existing results, the main contributions of these control strategies are maintaining the string stability in 1-D plane. The reliability of these approaches in the context of 2-D plane remains questionable. Moreover, the fast responses of a 2-D vehicle platoon system are necessary due to the more complicated working environment and control objectives. Therefore, when building the controller, the convergence time for distance tracking errors should be considered.

In addition to the distance keeping problem, the communication burden of the CACC control strategy should also be dealt with. One of the widely used techniques is the event-triggered control strategy in which the corresponding triggering mechanism can be constructed by fixed, relative, and dynamic threshold approaches [16]. Furthermore, to mitigate the impacts of system uncertainties and external disturbances, which are unavoidable in real-world systems, event-triggered control strategies are now being combined with several promising signal reconstruction techniques, such as the adaptive fuzzy logic system and the fuzzy observer-based method. According to the estimation results from the fuzzy observer, an adaptive backstepping event-triggered controller is proposed in [17] for the non-strict feedback system under the actuator faulty scenario. By noting the differentiation of the virtual controller in backstepping control, the event-triggered adaptive fuzzy control scheme integrating the dynamic surface mechanism is developed in [18] such that the path-following for the autonomous surface vessels can be realized. The proposed event-triggered controller in [19] with a relative threshold can ensure a fixed-time convergent performance for the vehicle suspension system. With the utilization of a modified relative-threshold triggering mechanism, the proposed adaptive fuzzy controller in [20] can not only maintain the multi-agent system's prescribed performance, but also release the communication burden between the controller and the actuator. By introducing a fuzzy observer and a time decaying event-triggering threshold, the distributed controller in [21] guarantees the consensus tracking performance of the nonlinear multi-agent system. Despite the availability of event-triggered control schemes in the literature for particular control issues, the event-triggered controller design for vehicle platoon systems with distance keeping limitations remains open and deserves to be further investigated. Therefore, this leads to the combination of the event-triggered control and the distance keeping control demand for constructing the controller in the present paper.

Motivated by the preceding discussions, the main objectives of the present paper can be divided into three parts, namely the problem formulation for fusion control of vehicle platoon systems in 2-D plane, the interval estimation-based unknown input reconstruction scheme, and the event-triggered distance keeping controller design. In particular, 2-D vehicle platoon systems are firstly proposed and the multi-lane fusion control problem for the vehicles spread in different lanes is interpreted as a stabilization problem of the tracking angle error between the adjacent vehicles. For the second part, an interval observer is proposed for the vehicle platoon systems. Based on the interval estimation, an unknown input reconstruction method is developed to asymptotically estimate the impact of the external disturbance and the system uncertainty for each vehicle. Thirdly, for maintaining the distance keeping constraints, an auxiliary tracking error is proposed with respect to a barrier function. By stabilizing the auxiliary tracking error, the distance keeping constraints are hence held. To achieve this, an adaptive fuzzy fusion controller is developed and the event-triggered mechanism is utilized so as to reduce the communication burden. The main contributions of the present paper are summarized as follows,

- Unlike the existing 1-D vehicle platoon control strategies [22], [23], the vehicle platoon control problem in the present paper is discussed within a 2-D plane. The multi-lane fusion control for the vehicle platoon has the potential to be applied to many actual driving scenarios, such as vehicles passing a tunnel.
- The interval estimation-based unknown input reconstruction can provide an asymptotic convergent estimation of the unknown input via algebraic calculation. Moreover, the reconstruction decouples the control input successfully. Consequently, it improves the flexibility for designing the controller with the unknown input compensation.
- To avoid the possible collision and loss of effective connection, the distance keeping criteria are put forward and they can be ensured by stabilizing an auxiliary tracking error generated from a barrier function. In contrast to [24], the distance tracking error in the present paper is constrained by a time decreasing boundary set and the error transformation process is simplified by the given barrier function when compared to $\arctan$ or $\log$ functions in [11]–[13]. In addition, the communication burden is eased by the event-triggered mechanism with a relative threshold.

The remainders of this paper are organized as follows. In Section II, the system description and some preliminaries are presented. The main results including the unknown input reconstruction and the controller design are given in Section III. Section IV provides the simulation results and the conclusion is summarized in Section V.

II. Problem Formulation and Preliminaries

A. System Dynamics

In this paper, vehicles are allowed to run in separate lanes. However, numerous lanes may merge into a single one in certain cases (e.g. when passing through a tunnel in Fig.1). Therefore, it is reasonable to assume that proper peripherals and GPS are mounted on each vehicle so as to acquire the positions of itself and its neighbors during the CACC manipulation. In addition, each vehicle is supposed to track its predecessor and this is also known as the predecessor following pattern. Therefore, the ith vehicle's control input is based on the $(i-1)$th vehicle's states and control input which are transferred wirelessly. The model for each follower vehicle is given as follows [24],

$$\begin{aligned}\dot{p}_{xi}(t) =& v_i(t)\cos\sigma_i(t),\ \dot{p}_{yi}(t) = v_i(t)\sin\sigma_i(t)\\ \dot{v}_i(t) =& a_i(t) = u_i(t) + s_i(p_{xi}, p_{yi}, v_i, t) + T_{di}(t)\\ \dot{\sigma}_i(t) =& \phi_i(t),\ \dot{\phi}_i(t) = \tau_i(t),\ i = 1,\ldots,N\end{aligned} \tag{1}$$

where p_{xi}, p_{yi} are the absolute position along with the orthogonal axises in a two dimensional coordinate axis. v_i is the volume of vehicle's velocity. σ_i stands for the angle between the vehicle's headway direction and the positive X-axis. In other words, σ_i represents the direction of vehicle's velocity. u_i is the control input of each vehicle. ϕ_i is the acceleration of σ_i. τ_i is the time-derivative of ϕ_i, representing the other control variable. $s_i(p_{xi}, p_{yi}, v_i, t)$ is the nonlinear part of the vehicle system including unmodeled system dynamics such as the aerodynamic drags, rolling and gradient resistances. T_{di} is the external disturbance for each vehicle. In this paper, the impacts of the external disturbance and the unmodeled system dynamics have been lumped together and the corresponding unknown input S_{id} is defined as $S_{id} = s_i + T_{di}$.

As for the leader which is labeled as Vehicle 0, the dynamic model is given as [24],

$$\begin{aligned} \dot{p}_{x0}(t) =& v_0(t)\cos\sigma_0(t),\ \dot{p}_{y0}(t) = v_0(t)\sin\sigma_0(t) \\ \dot{v}_0(t) =& a_0(t) \end{aligned} \tag{2}$$

In this paper, vehicle 0 is considered as a virtual leader which is an ideal vehicle and free from system uncertainty and disturbance. All the vehicles are assumed traveling alongside the positive X-axis in the same direction. Moreover, for simplicity, the virtual leader is considered to remain in a single lane with no need to change lanes, and so its velocity angle σ_0 is 0.

Assumption 1 ([24]). *The external disturbance $T_{di}(t)$ is bounded such that $|T_{di}(t)| \leq T_d$ where T_d is known.*

Assumption 2. *The unknown nonlinear part s_i is bounded such that $|s_i| \leq S$ where S is known.*

Remark 1. *The model proposed in [24] and the present paper for the vehicle platoon is a simplified version of the real vehicle. Moreover, this vehicle model is constructed on the basis of the commonly used vehicle model in [25]–[27]. Traditional 1-D platoon control in [25]–[27] can be subsumed under the 2-D problem addressed in this paper with the velocity deflection angle $\sigma_i(t) = 0$. Furthermore, the variation range for the velocity angle is set as $\sigma_i \in [-\pi, \pi]$.*

Remark 2. *It notes that Assumption 1-2 require the boundaries T_d and S in advance. These variables may vary from vehicles to vehicles. Even though T_d and S are hard to be obtained accurately in practice, the subsequent unknown input reconstruction method can fix this problem because different selections of the boundaries for T_d and S result in almost the same unknown reconstruction performances, just as claimed in Remark 4.*

B. Problem Formulation

According to Fig.1, vehicles distributed over multiple lanes are forced to merge into one lane due to some special road conditions. The communication topology of the vehicle platoon is illustrated in Fig.2. Moreover, to avoid the collision and loss of effective communication, the distance keeping should be addressed carefully during the vehicular fusion process. In this paper, a constant distance keeping policy is adopted. The

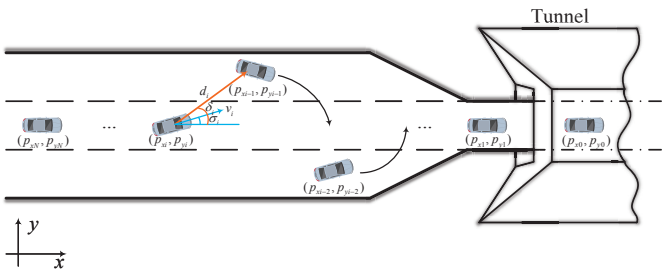

Fig. 1. The structure of the 2-D vehicle platoon when passing through tunnel.

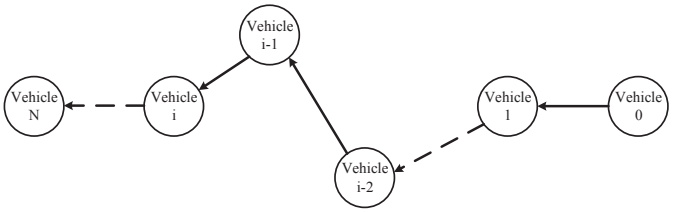

Fig. 2. The communication topology of the 2-D vehicle platoon.

actual gap $d_i(t)$ and the relative position angle $\delta_i(t)$ between the ith vehicle and its predecessor is given as,

$$d_i(t) = \sqrt{(p_{xi-1} - p_{xi})^2 + (p_{yi-1} - p_{yi})^2} \tag{3}$$

$$\delta_i(t) = \text{atan2}\left[(p_{yi-1} - p_{yi}), (p_{xi-1} - p_{xi})\right] \tag{4}$$

The distance constraints for each follower are defined as,

$$0 < \mathscr{D}_{col} < d_i(t) < \mathscr{D}_{con} \tag{5}$$

where $\mathscr{D}_{col}$ stands for the minimum collision avoidance gap and $\mathscr{D}_{con}$ indicates the maximum effective communication range. Moreover, it is assumed that the initial distance gap between each adjacent vehicles is within the effective communication range. Therefore, it is possible to propose a proper distance keeping controller which is constructed on the shared states among the adjacent vehicles.

Remark 3. *Although the communication reliability may be affected by various factors, the effective communication is defined to be only related to the distance of the adjacent vehicles in the present paper. It means that the reliable communication can be obtained within the limited communication range.*

To realize the multi-lane vehicle fusion, we define,

$$e_i(t) = d_i(t) - d \tag{6}$$

$$e_{\sigma_i}(t) = \sigma_i(t) - \delta_i(t) \tag{7}$$

where d is the target inter-vehicular distance imposed by the constant distance keeping policy. Furthermore, it has $\Delta_l < e_i(t) < \Delta_u$ where $\Delta_l = \mathscr{D}_{col} - d$ and $\Delta_u = \mathscr{D}_{con} - d$. Then, based on (3), and (6), the time derivative for $e_i(t)$ is given as,

$$\dot{e}_i = \eta_{i1}(t)v_i(t) + \eta_{i2}(t)$$

where

$$\begin{aligned} \eta_{i1}(t) =& -\left[\cos\sigma_i\,(p_{xi-1} - p_{xi}) + (p_{yi-1} - p_{yi})\sin\sigma_i\right]/d_i(t) \\ \eta_{i2}(t) =& \left[(p_{xi-1} - p_{xi})\,v_{i-1}\cos\sigma_{i-1}\right. \\ & \left. + (p_{yi-1} - p_{yi})\,v_{i-1}\sin\sigma_{i-1}\right]/d_i(t) \end{aligned}$$

According to the above discussion, the main concerns can be categorized as follows,

- Designing a distance constraints-based backstepping fusion controller for each follower vehicle so as to keep the desired distance gap d and realize the multi lane fusion.
- To eliminate the influences caused by the unmodeled system dynamics and the external disturbance, an asymptotic convergent unknown input reconstruction method is developed based on state interval estimation.
- Because of the limited on-board communication resources, the event-trigger-based control strategy is introduced to the proposed controller.

Based on this understanding, the control structure in the present paper is depicted in Fig.3. The following lemmas are introduced before proceeding with the controller design.

Lemma 1 ([28]). *If a Lyapunov function $V(x(t))$ holds $\dot{V}(x(t)) \leq b_1 V^{a_1}(x(t)) - b_2 V^{a_2}(x(t)) + \aleph$ where $b_1 > 0$, $b_2 > 0$, $\aleph > 0$, $a_1 \in (0,1)$ and $a_2 \in (1,\infty)$, then all the signals in the system converge to the following residual set within a fixed setting time t_r,*

$$\mathscr{R} = \left\{ x(t) | V \leq \min \left\{ b_1^{\frac{-1}{a_1}} \left(\frac{\aleph}{1-l} \right)^{\frac{1}{a_1}}, b_2^{\frac{-1}{a_2}} \left(\frac{\aleph}{1-l} \right)^{\frac{1}{a_2}} \right\} \right\}$$

where $l \in (0,1)$ and the setting time T_r holds,

$$t_r \leq t_{r,max} = \frac{1}{b_1 l (1-a_1)} + \frac{1}{b_2 l (a_2 - 1)}$$

Lemma 2 ([29]). *For $\forall \varkappa \in \mathcal{R}$ and $\aleph > 0$, it can be concluded that $0 \leq |\varkappa| - \varkappa \tanh(\varkappa/\aleph) \leq 0.2785\aleph$.*

Lemma 3 ([30]). *For b_1, $b_2 \in \mathcal{R}$, it holds that*

$$|b_1|^{a_1} |b_2|^{a_2} \leq \frac{a_1}{a_1 + a_2} \varkappa |b_1|^{a_1 + a_2} + \frac{a_2}{a_1 + a_2} \varkappa^{-\frac{a_1}{a_2}} |b_2|^{a_1 + a_2}$$

where a_1, a_2 and $\varkappa$ are positive constants.

Lemma 4 ([28]). *For $\varkappa_j \geq 0$, then it has,*

$$\sum_{j=1}^{n} \varkappa_j^{a_1} \geq \left(\sum_{j=1}^{n} \varkappa_j \right)^{a_1}, \ 0 < a_1 \leq 1$$

$$n^{1-a_2} \left(\sum_{j=1}^{n} \varkappa_j \right)^{a_2} \leq \sum_{j=1}^{n} \varkappa_j^{a_2} \leq \left(\sum_{j=1}^{n} \varkappa_j \right)^{a_2}, \ 1 < a_2 \leq \infty$$

Lemma 5 ([30]). *For $\varkappa \in \mathcal{R}$ and $\forall \aleph > 0$, it has $0 \leq |\varkappa| < \aleph + \varkappa^2 / \sqrt{\varkappa^2 + \aleph^2}$.*

Lemma 6 ([31]). *For a continuous function $F(x)$, there exists a fuzzy logic system such that,*

$$\sup_{x \in \mathcal{X}} \left| F(x) - W^T \varphi(x) \right| \leq h(x)$$

where x stands for the input and the ideal weight vector is defined as $W = [w_1, \ldots, w_l]^T \in \mathcal{R}^l$. The approximation error holds $|h(x)| < \hbar$. The fuzzy basis function $\varphi(x)$ is chosen as $\varphi(x) = [\varphi_1(x), \ldots, \varphi_l(x)]^T / \sum_{j=1}^{l} \varphi_j(x)$ in which $\varphi_j(x) = exp\left[-\frac{(x - \mathscr{C}_j)^T (x - \mathscr{C}_j)}{\mathscr{W}_j^2} \right]$ where $j = 1, \ldots, l$, $\mathscr{C}_j$ is the center of $\varphi_j(x)$ and $\mathscr{W}_j$ is the width of $\varphi_j(x)$.

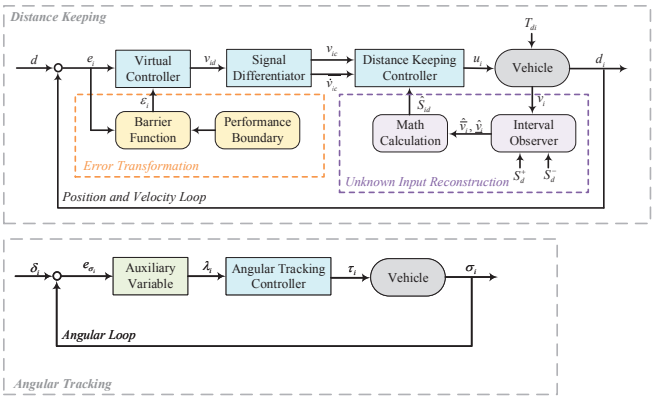

Fig. 3. The control structure for the vehicles in 2-D vehicle platoon.

III. Main Results

A. Unknown Input Reconstruction

To offset the external disturbance and the unknown modeled system dynamics, an unknown input reconstruction strategy is proposed. For this purpose, an interval observer is firstly presented as follows,

$$\dot{\hat{v}}_i(t) = u_i(t) + S_d^+ - S_d^- - L_i \left(v_i - \hat{v}_i \right) \tag{8}$$

$$\dot{\underline{v}}_i(t) = u_i(t) + S_d^- - S_d^+ - L_i \left(v_i - \underline{v}_i \right) \tag{9}$$

where L_i is the observer gain and it can be any negative constants, $S_d^+ = S + T_d$ and $S_d^- = -S_d^+$. $\hat{v}_i$ and $\underline{v}_i$ are the upper and lower boundary estimations of v_i.

Theorem 1. *According to the interval observer (8) and (9), if the initial states satisfy that $\underline{v}_i(0) < v_i(0) < \hat{v}_i(0)$, then $\underline{v}_i(t) < v_i(t) < \hat{v}_i(t)$ holds for all $t \geq 0$.*

Proof: Firstly, the estimation errors are defined as $\tilde{\hat{v}}_i = \hat{v}_i - v_i$ and $\tilde{\underline{v}}_i = v_i - \underline{v}_i$. Then we have,

$$\dot{\tilde{\hat{v}}}_i = L_i \tilde{\hat{v}}_i + S_d^+ - S_d^- - S_{id}(t)$$

$$\dot{\tilde{\underline{v}}}_i = L_i \tilde{\underline{v}}_i - S_d^- + S_d^+ + S_{id}(t)$$

It is easy to show that $S_d^+ - S_d^- - S_{id}(t) > 0$ and $-S_d^- + S_d^+ + S_{id}(t) > 0$. As a result, if $\underline{v}_i(0) < v_i(0) < \hat{v}_i(0)$, then $\underline{v}_i(t) < v_i(t) < \hat{v}_i(t)$ always holds. ■

Furthermore, there always exists $\ell_i(t) \in (0,1)$ such that,

$$v_i(t) = \ell_i(t) \hat{v}_i(t) + (1 - \ell_i(t)) \, \underline{v}_i(t) \tag{10}$$

By noting (8)-(10), it has,

$$\begin{aligned} \dot{\hat{v}}_i &= u_i + S_d^+ - S_d^- - L_i \left[\ell_i \hat{v}_i + (1 - \ell_i) \, \underline{v}_i - \hat{v}_i \right] \\ &= \mathscr{G}_{i1} \hat{v}_i - \mathscr{G}_{i1} \underline{v}_i + u_i + S_d^+ - S_d^- \end{aligned} \tag{11}$$

$$\begin{aligned} \dot{\underline{v}}_i &= u_i + S_d^- - S_d^+ - L_i \left[\ell_i \hat{v}_i + (1 - \ell_i) \, \underline{v}_i - \underline{v}_i \right] \\ &= \mathscr{G}_{i2} \hat{v}_i - \mathscr{G}_{i2} \underline{v}_i + u_i + S_d^- - S_d^+ \end{aligned} \tag{12}$$

where $\mathscr{G}_{i1} = -L_i (\ell_i - 1)$ and $\mathscr{G}_{i2} = -L_i \ell_i$. Referring to (10)-(12), we can have,

$$\begin{aligned} \dot{v}_i =& \left[(1 - \ell_i) \mathscr{G}_{i2} + \dot{\ell}_i + \ell_i \mathscr{G}_{i1} \right] \hat{v}_i + (2\ell_i - 1) \, S_d^+ \\ &+ \left[-(1 - \ell_i) \mathscr{G}_{i2} - \ell_i \mathscr{G}_{i1} - \dot{\ell}_i \right] \underline{v}_i - (2\ell_i - 1) \, S_d^- + u_i \\ =& u_i + \Xi_{i1} \left(\hat{v}_i - \underline{v}_i \right) + \Xi_{i2} \left(S_d^+ - S_d^- \right) \end{aligned} \tag{13}$$

where $\Xi_{i1} = \ell_i \mathscr{G}_{i1} + \dot{\ell}_i + (1-\ell_i)\mathscr{G}_{i2}$ and $\Xi_{i2} = 2\ell_i - 1$. By comparing (13) with (1), the unknown input S_{id} can be represented as,

$$S_{id} = \Xi_{i1}\left(\hat{\bar{v}}_i - \hat{\underline{v}}_i\right) + \Xi_{i2}\left(S_d^+ - S_d^-\right) \tag{14}$$

According to (13), the derivation of ℓ_i is used. To acquire $\dot{\ell}_i$, we firstly rewritten (10) as,

$$\ell_i = \left(v_i - \hat{\underline{v}}_i\right) / \left(\hat{\bar{v}}_i - \hat{\underline{v}}_i\right) \tag{15}$$

By passing ℓ_i through the differentiator in [32], then the estimate of $\dot{\ell}_i$, which is denoted by $\hat{\dot{\ell}}_i$, can be acquired within a fixed time. Moreover, based on (14), the unknown input reconstruction result is presented as,

$$\hat{S}_{id} = \hat{\Xi}_{i1}\left(\hat{\bar{v}}_i - \hat{\underline{v}}_i\right) + \Xi_{i2}\left(S_d^+ - S_d^-\right) \tag{16}$$

where $\hat{\Xi}_{i1} = \ell_i \mathscr{G}_{i1} + \hat{\dot{\ell}}_i + (1-\ell_i)\mathscr{G}_{i2}$.

Remark 4. *Based on the interval estimations from the interval observer (8) and (9), an algebraic relationship between the unknown input of S_{id} and v_i is established. Moreover, by referring to the algebraic relationship in (14), an unknown input reconstruction method is hence developed in (16). The proposed unknown input reconstruction possesses some significant features. Firstly, it is an algebraic reconstruction and it can estimate the actual S_{id} asymptotically. Secondly, the reconstruction result decouples the control input signal u_i successfully. Therefore, designing a controller with the unknown input compensation becomes possible. Thirdly, although the unknown input reconstruction (16) relies on the values of S_d^+ and S_d^-, different boundary selections result in almost the same reconstructions.*

B. Event-triggered Fixed-time Multi-Lane Fusion Control with Distance Constraints

From (5) and (6), we can notice that the distance constraints are expressed as an interval with fixed boundaries. To improve the tracking performance and the accuracy, the distance constraints are modified as,

$$\Delta_l \le \Delta_{il}(t) < e_i(t) < \Delta_{iu}(t) \le \Delta_u \tag{17}$$

Moreover, $\Delta_{il}(t)$ and $\Delta_{iu}(t)$ in (17) are defined as,

$$\begin{aligned}\Delta_{il}(t) &= -(\Delta_{il\infty} - \Delta_l)\exp(-\varsigma_{il}t) + \Delta_{il\infty}\\ \Delta_{iu}(t) &= (\Delta_u - \Delta_{iu\infty})\exp(-\varsigma_{iu}t) + \Delta_{iu\infty}\end{aligned}$$

where $\Delta_{il\infty}$ and $\Delta_{iu\infty}$ satisfying $\Delta_{il\infty} < 0 < \Delta_{iu\infty}$ are the predesigned ultimate values for $\Delta_{il}(t)$ and $\Delta_{iu}(t)$. The positive parameters ς_{il} and ς_{iu} are the damping ratios for $\Delta_{il}(t)$ and $\Delta_{iu}(t)$. Selecting constant $\bar{\Delta}_{il}$ and $\underline{\Delta}_{iu}$ such that,

$$\Delta_{il}(t) < \bar{\Delta}_{il},\ \underline{\Delta}_{iu} < \Delta_{iu}(t)$$

To convert (17) into an unconstrained expression, the following barrier function is developed,

$$\begin{aligned}\varepsilon_i &= \frac{e_i(t) - \bar{\Delta}_{il}}{e_i(t) - \Delta_{il}(t)} + \frac{e_i(t) - \underline{\Delta}_{iu}}{\Delta_{iu}(t) - e_i(t)}\\ &= \varepsilon_{i1} e_i(t) + \varepsilon_{i2}\end{aligned} \tag{18}$$

where $\varepsilon_{i1} = \frac{\bar{\Delta}_{il} - \Delta_{il} + \Delta_{iu} - \underline{\Delta}_{iu}}{(e_i(t) - \Delta_{il})(\Delta_{iu} - e_i(t))}$ and $\varepsilon_{i2} = \frac{\Delta_{il}\underline{\Delta}_{iu} - \bar{\Delta}_{il}\Delta_{iu}}{(e_i(t) - \Delta_{il})(\Delta_{iu} - e_i(t))}$. Moreover, the derivative of ε_i is $\dot{\varepsilon}_i = \zeta_{i1}\dot{e}_i(t) + \zeta_{i2}$ where $\zeta_{i1} = \frac{\bar{\Delta}_{il} - \Delta_{il}}{(e_i - \Delta_{il})^2} + \frac{\Delta_{iu} - \underline{\Delta}_{iu}}{(\Delta_{iu} - e_i)^2}$ and $\zeta_{i2} = \frac{\left(e_i - \bar{\Delta}_{il}\right)\dot{\Delta}_{il}}{(e_i - \Delta_{il})^2} - \frac{\left(e_i - \underline{\Delta}_{iu}\right)\dot{\Delta}_{iu}}{(\Delta_{iu} - e_i)^2}$. According to (18), $\varepsilon_i \to +\infty$ when $e_i(t) \to \Delta_{iu}(t)^-$ and $\varepsilon_i \to -\infty$ when $e_i(t) \to \Delta_{il}(t)^+$. Moreover, to perform an accurate tracking performance by maintaining the fixed distance gap d, the ideal form for ε_i is chosen as ε_{id},

$$\varepsilon_{id} = \left(\bar{\Delta}_{il}\Delta_{iu} - \Delta_{il}\underline{\Delta}_{iu}\right) / \left(\Delta_{il}\Delta_{iu}\right) \tag{19}$$

The time derivative of ε_{id} is calculated as follows,

$$\dot{\varepsilon}_{id} = -\bar{\Delta}_{il}\dot{\Delta}_{il}/\Delta_{il}^2 + \underline{\Delta}_{iu}\dot{\Delta}_{iu}/\Delta_{iu}^2 = \zeta_{i3}$$

The error between ε_i and ε_{id} is defined as $z_{i1} = \varepsilon_i - \varepsilon_{id}$. Referring to (18) and (19), we have,

$$\begin{aligned}\dot{z}_{i1} &= \zeta_{i1}\dot{e}_i(t) + \zeta_{i2} - \zeta_{i3}\\ &= \zeta_{i1}\eta_{i1}v_i(t) + \zeta_{i1}\eta_{i2} + \zeta_{i2} - \zeta_{i3}\\ &= \chi_{i1}v_i(t) + \chi_{i2}\end{aligned}$$

where $\chi_{i1} = \zeta_{i1}\eta_{i1}$ and $\chi_{i2} = \zeta_{i1}\eta_{i2} + \zeta_{i2} - \zeta_{i3}$. Up to now, it notes that the time-varying performance constraints for the tracking error $e_i(t)$ can be maintained by stabilizing z_{i1}.

Remark 5. *Unlike the output constrained control approach in [24], the proposed distance constraint control scheme can provide a dynamic output constraint boundary whereas in [24], the constraint boundaries are set as fixed or symmetric ones via a given barrier Lyapunov function. Moreover, although some modifications for the fixed boundary can be found in [33] with the utilization of the integral-type Lyapunov function, the upper and lower boundaries of the tracking error are symmetric. Therefore, the asymmetric boundary set can be viewed as another merit of the proposed method. In addition, differing from* $\arctan$ *or* $\log$ *functions in [11]–[13], the error transformation is simplified by a given barrier function in (18) which can be viewed as the extension of [11]–[13].*

To show the convergence of z_{i1}, we construct a Lyapunov candidate function as $V_1 = \sum_{i=1}^{N} \frac{1}{2} z_{i1}^2$ and the time derivative of V_1 holds,

$$\begin{aligned}\dot{V}_1 &= \sum_{i=1}^{N}\left[z_{i1}\left(\chi_{i1}v_i(t) + \chi_{i2}\right)\right]\\ &= \sum_{i=1}^{N}\left\{z_{i1}\left[\chi_{i1}\left(v_{id0}(t) + z_{i2d}\right) + \chi_{i2}\right]\right\}\end{aligned} \tag{20}$$

where $v_{id0}(t)$ is known as the virtual controller for z_{i1} and $z_{i2d} = v_i - v_{id0}$. According to (20), a fixed-time virtual controller is constructed as follows,

$$v_{id0} = \frac{1}{\chi_{i1}}\left(-\chi_{i2} - c_{i1}z_{i1}^{2q_1-1} - c_{i2}z_{i1}^{2q_2-1}\right) \tag{21}$$

where $c_{i1} > 0$, $c_{i2} > 0$, $0 < q_1 < 1$ and $q_2 > 1$. Substituting (21) into (20) yields,

$$\begin{aligned}\dot{V}_1 \le &-2^{q_1}\min\left\{c_{i1}\right\}V_1^{q_1} + \sum_{i=1}^{N} z_{i1}\chi_{i1}z_{i2d}\\ &-2^{q_2}\min\left\{c_{i2}\right\}N^{1-q_2}V_1^{q_2}\end{aligned}$$

According to Lemma 1, if z_{i2d} is asymptotically convergent, then the fixed-time convergence for z_{i1} is achieved. Moreover, based on the backstepping control framework, the derivation of the virtual controller is necessary and the signal differentiator in [32] is deployed here. However, the estimation error is inevitable in the presence of the differentiator. Then the virtual controller is modified as v_{id} and the estimation error is defined as $z_{i2\Delta} = v_{ic} - v_{id}$ where v_{ic} is the estimate of v_{id} from the differentiator. Consequently, we have,

$$\begin{aligned}\dot{V}_1 =& \sum_{i=1}^{N} \{z_{i1} [\chi_{i1} (v_i - v_{ic} + v_{ic} - v_{id} + v_{id}) + \chi_{i2}]\} \\ =& \sum_{i=1}^{N} \{z_{i1} [\chi_{i1} (z_{i2} + z_{i2\Delta} + v_{id}) + \chi_{i2}]\} \end{aligned} \tag{22}$$

where $z_{i2} = v_i - v_{ic}$. According to (22), the adaptive fuzzy fixed-time virtual controller is given as,

$$v_{id} = \frac{1}{\chi_{i1}} \left(-\chi_{i2} - c_{i1} z_{i1}^{2q_1 - 1} - c_{i2} z_{i1}^{2q_2 - 1} - \frac{1}{2\kappa_{i1}} z_{i1} \hat{\theta}_i \varphi_i^T \varphi_i \right) \tag{23}$$

$$\dot{\hat{\theta}}_i = \frac{\gamma_i}{2\kappa_{i1}} z_{i1}^2 \varphi_i^T \varphi_i - \beta_i \hat{\theta}_i \tag{24}$$

where γ_i, κ_{i1} and β_i are positive constants. φ_i is the fuzzy basis function vector and $\hat{\theta}_i$ is the parameter in fuzzy system which will be designed later.

Remark 6. *In some output control strategies like [34], the variables to be constrained are the compound of the tracking error and the errors generated by the command filter. Therefore, the real constraint for the tracking error cannot be guaranteed directly. In the present paper, this problem has been solved. Moreover, the adaptive fuzzy process is used to compensate the errors between the ideal virtual controller v_{id} and the command filtered controller v_{ic}.*

Remark 7. *By noting the definition of η_{i1}, χ_{i1} and v_{id}, the singularity problem may occur when the vehicles share the same X position and $\sigma_i = 0$. Therefore, the applicable situation for the proposed control strategy requires the vehicles possess different X positions at the initial time.*

Remark 8. *It should be noticed that the computational complexity of the adaptive fuzzy virtual controller is related to the number of fuzzy rules, the adaptive process of the parameters and the control signals. (23) and (24) show that only one adaptive parameter and one virtual controller need to be updated. Therefore, one way to further reduce the computational complexity of the controller design is to select the proper fuzzy rules and constrain the total number of the fuzzy rules with respect to the detailed application environment.*

By referring (23) and (24), we design $V_{1,m} = V_1 + \sum_{i=1}^{N} \frac{1}{2\gamma_i} \tilde{\theta}_i^2$ where $\tilde{\theta}_i = \theta_i - \hat{\theta}_i$. Then $\dot{V}_{1,m}$ holds,

$$\begin{aligned}\dot{V}_{1,m} =& \sum_{i=1}^{N} (z_{i1}\chi_{i1} z_{i2} + z_{i1}\chi_{i1} z_{i2\Delta} + z_{i1}\chi_{i1} v_{id} + z_{i1}\chi_{i2}) \\ &+ \sum_{i=1}^{N} \left(-\frac{1}{\gamma_i} \tilde{\theta}_i \dot{\hat{\theta}}_i + \frac{1}{2\kappa_{i2}} z_{i1}^2 - \frac{1}{2\kappa_{i2}} z_{i1}^2 \right) \end{aligned} \tag{25}$$

In addition, we define $\alpha_i = \chi_{i1} z_{i2\Delta} + \frac{1}{2\kappa_{i2}} z_{i1}$. Based on the fuzzy logic system in Lemma 6, it can be obtained that,

$$\alpha_i = W_i^T \varphi(z_{i1}) + \hbar_i(z_{i1}), \ |\hbar_i(z_{i1})| \le \hbar$$

where W_i is the ideal weight vector and $\theta_i = W_i^T W_i$. $\hbar_i(z_{i1})$ is a bounded estimation error. Furthermore, we have,

$$z_{i1}\alpha_i \le \frac{1}{2\kappa_{i1}} z_{i1}^2 \theta_i \varphi_i^T \varphi_i + \frac{\kappa_{i1}}{2} + \frac{1}{2\kappa_{i2}} z_{i1}^2 + \frac{1}{2}\kappa_{i2}\hbar^2$$

Substituting (23) and (24) into (25) gives,

$$\begin{aligned}\dot{V}_{1,m} \le& \sum_{i=1}^{N} \Bigg(z_{i1}\chi_{i1} z_{i2} + \frac{1}{2\kappa_{i1}} z_{i1}^2 \theta_i \varphi_i^T \varphi_i + \frac{\kappa_{i1}}{2} + \frac{1}{2}\kappa_{i2}\hbar^2 \\ &+ z_{i1}\chi_{i2} + \frac{1}{2\kappa_{i2}} z_{i1}^2 - z_{i1}\chi_{i2} - c_{i1} z_{i1}^{2q_1} - c_{i2} z_{i1}^{2q_2} \\ &- \frac{1}{2\kappa_{i1}} z_{i1}^2 \hat{\theta}_i \varphi_i^T \varphi_i - \frac{1}{2\kappa_{i2}} z_{i1}^2 \Bigg) \\ &+ \sum_{i=1}^{N} \left(-\frac{1}{2\kappa_{i1}} z_{i1}^2 \tilde{\theta}_i \varphi_i^T \varphi_i + \frac{\beta_i}{\gamma_i} \tilde{\theta}_i \hat{\theta}_i \right) \end{aligned} \tag{26}$$

Noting Lemma 3 and the fact that $\frac{\beta_i}{\gamma_i} \tilde{\theta}_i \hat{\theta}_i \le -\frac{\beta_i}{2\gamma_i} \tilde{\theta}_i^2 + \frac{\beta_i}{2\gamma_i} \theta_i^2$, if we set $b_1 = 1$, $b_2 = \frac{1}{2\gamma_i} \tilde{\theta}_i^2$, $a_1 = 1 - q_1$, $a_2 = q_1$, and $\varkappa = \exp\left(\frac{q_1}{1-q_1} \log q_1 \right)$, then it has $-\frac{1}{2\gamma_i} \tilde{\theta}_i^2 \le -\left(\frac{1}{2\gamma_i} \tilde{\theta}_i^2 \right)^{q_1} + (1 - q_1) q_1^{\frac{q_1}{1-q_1}}$. Similarly, we can have, $-\frac{1}{2\gamma_i} \tilde{\theta}_i^2 \le -\left(\frac{1}{2\gamma_i} \tilde{\theta}_i^2 \right)^{q_2} + (1 - q_2) q_2^{\frac{q_2}{1-q_2}}$. Based on the above deduction, (26) holds,

$$\begin{aligned}\dot{V}_{1,m} \le& \sum_{i=1}^{N} \left(z_{i1}\chi_{i1} z_{i2} + \frac{\kappa_{i1}}{2} + \frac{1}{2}\kappa_{i2}\hbar^2 - c_{i1} z_{i1}^{2q_1} - c_{i2} z_{i1}^{2q_2} \right) \\ &+ \sum_{i=1}^{N} \Bigg[\frac{\beta_i}{2\gamma_i} \theta_i^2 - \frac{\beta_i}{2} \left(\frac{1}{2\gamma_i} \tilde{\theta}_i^2 \right)^{q_1} \\ &+ \frac{\beta_i}{2} (1 - q_1) q_1^{\frac{q_1}{1-q_1}} - \frac{\beta_i}{2} \left(\frac{1}{2\gamma_i} \tilde{\theta}_i^2 \right)^{q_2} \Bigg] \\ \le& - G_1 V_1^{q_1} - G_2 V_1^{q_2} + \sum_{i=1}^{N} z_{i1}\chi_{i1} z_{i2} + \Delta_{V_1} \end{aligned} \tag{27}$$

where

$$\Delta_{V_1} = \sum_{i=1}^{N} \left(\frac{\kappa_{i1}}{2} + \frac{\kappa_{i2}}{2}\hbar^2 + \frac{\beta_i}{2\gamma_i}\theta_i^2 + \frac{\beta_i}{2}(1 - q_1) q_1^{\frac{q_1}{1-q_1}} \right),$$

$$G_1 = \min\left\{ 2^{q_1} c_{i1}, \frac{\beta_i}{2} \right\}, \ G_2 = N^{1-q_2} \min\left\{ 2^{q_2} c_{i2}, \frac{\beta_i}{2} \right\}.$$

To stabilize z_{i2}, the relative threshold event-triggered mechanism is introduced. Firstly, the system dynamic is transformed into $\dot{v}_i = u_i(t) + S_{id}(t)$. Moreover, the relative threshold event-triggering mechanism is given as,

$$u_{io}(t) = u_{ic}\left(t_{k_i}^i \right), \ \forall t \in \left[t_{k_i}^i, t_{k_{i+1}}^i \right) \tag{28}$$

$$t_{k_{i+1}}^i = \inf\left\{ t > t_{k_i}^i \,||E_i(t)| \ge \vartheta_{i1}|u_{io}(t)| + \vartheta_{i2} \right\} \tag{29}$$

where $u_{io}(t)$ is an intermediate control variable, $0 < \vartheta_{i1} < 1$ and $\vartheta_{i2} > 0$, $E_i(t) = u_{ic}(t) - u_{io}(t)$. $t_{k_i}^i$ is the latest triggering time point of the ith vehicle. From (28) and (29), we have,

$$|E_i(t)| = |u_{ic}(t) - u_{io}(t)| < \vartheta_{i1}|u_{io}(t)| + \vartheta_{i2}, \ \forall t \in \left[t_{k_i}^i, t_{k_{i+1}}^i \right)$$

Then $u_{ic}(t) = (1+\psi_{i1}(t)\vartheta_{i1})\,u_{io}(t) + \psi_{i2}(t)\vartheta_{i2}$ where $|\psi_{i1}(t)| \leq 1$ and $|\psi_{i2}(t)| \leq 1$. Consequently, it has,

$$u_{io}(t) = \frac{u_{ic}(t)}{1+\psi_{i1}(t)\vartheta_{i1}} - \frac{\psi_{i2}(t)\vartheta_{i2}}{1+\psi_{i1}(t)\vartheta_{i1}} \tag{30}$$

Based on (28)-(30), the controller is designed as,

$$u_i = -\frac{z_{i2}u_{io}^2}{\sqrt{z_{i2}^2u_{io}^2+\Upsilon_i^2}} \tag{31}$$

$$u_{ic} = (1+\vartheta_{i1})\left[\mathscr{L}_i \tanh\left(\frac{z_{i2}\mathscr{L}_i}{\varsigma_{i1}}\right) + \bar{\vartheta}_{i1}\tanh\left(\frac{z_{i2}\bar{\vartheta}_{i1}}{\varsigma_{i1}}\right)\right] \tag{32}$$

where $\mathscr{L}_i = \hat{S}_{id} - \dot{v}_{ic} + c_{i3}z_{i2}^{2q_1-1} + c_{i4}z_{i2}^{2q_2-1} + \chi_{i1}z_{i1}$ and $\bar{\vartheta}_{i1} > \vartheta_{i2}/(1-\vartheta_{i1})$. c_{i3}, c_{i4}, Υ_i and ς_{i1} are positive constants. Then we have the following theorem.

Theorem 2. *Considering the given 2-D platoon system in (1), the proposed event-triggered backstepping controller (31) and (32) with virtual controller in (23) can ensure the distance keeping constraints in (5) and the fixed time convergence of the tracking error in (17).*

Proof: Firstly, the Lyapunov candidate is chosen as $V_2 = V_{1,m} + \sum_{i=1}^{N}\frac{1}{2}z_{i2}^2$. Based on Lemma 5, $\dot{V}_2$ holds,

$$\begin{aligned}
\dot{V}_2 &= \dot{V}_{1,m} + \sum_{i=1}^{N}\left(-\frac{z_{i2}^2u_{io}^2}{\sqrt{z_{i2}^2u_{io}^2+\Upsilon_i^2}} + z_{i2}S_{id} - z_{i2}\dot{v}_{ic}\right)\\
&\leq \dot{V}_{1,m} + \sum_{i=1}^{N}\left(\Upsilon_i - z_{i2}u_{io} + z_{i2}S_{id} - z_{i2}\dot{v}_{ic}\right)\\
&\leq \dot{V}_{1,m} + \sum_{i=1}^{N}\left(-\frac{z_{i2}u_{ic}}{1+\vartheta_{i1}} + \left|\frac{z_{i2}\vartheta_{i2}}{1-\vartheta_{i1}}\right| + z_{i2}S_{id} - z_{i2}\dot{v}_{ic}\right)\\
&+ \sum_{i=1}^{N}\left(\Upsilon_i + c_{i3}z_{i2}^{2q_1} + c_{i4}z_{i2}^{2q_2} - c_{i3}z_{i2}^{2q_1} - c_{i4}z_{i2}^{2q_2}\right)
\end{aligned} \tag{33}$$

According to Lemma 2, it holds that,

$$\begin{aligned}
z_{i2}\mathscr{L}_i \leq& |z_{i2}\mathscr{L}_i| \leq z_{i2}\mathscr{L}_i\tanh\left(z_{i2}\mathscr{L}_i/\varsigma_{i1}\right) + 0.2785\varsigma_{i1}\\
z_{i2}\bar{\vartheta}_{i1} \leq& |z_{i2}\bar{\vartheta}_{i1}| \leq z_{i2}\bar{\vartheta}_{i1}\tanh\left(z_{i2}\bar{\vartheta}_{i1}/\varsigma_{i1}\right) + 0.2785\varsigma_{i1}
\end{aligned}$$

Substituting (32) into (33), it has,

$$\begin{aligned}
\dot{V}_2 \leq& \sum_{i=1}^{N}\left(-c_{i1}z_{i1}^{2q_1} - c_{i2}z_{i1}^{2q_2} - c_{i3}z_{i2}^{2q_1} - c_{i4}z_{i2}^{2q_2}\right)\\
&- \sum_{i=1}^{N}\left[\frac{\beta_i}{2}\left(\frac{1}{2\gamma_i}\tilde{\theta}_i^2\right)^{q_1} + \frac{\beta_i}{2}\left(\frac{1}{2\gamma_i}\tilde{\theta}_i^2\right)^{q_2}\right] + \Delta_{V_2}\\
\leq& -G_3V_2^{q_1} - G_4V_2^{q_2} + \Delta_{V_2}
\end{aligned} \tag{34}$$

where $\Delta_{V_2} = \sum_{i=1}^{N}(\Upsilon_i + 0.557\varsigma_{i1}) + \Delta_{V_1}$, $G_3 = \min\left\{2^{q_1}c_{i1}, 2^{q_1}c_{i3}, \frac{\beta_i}{2}\right\}$, $G_4 = N^{1-q_2}\min\left\{2^{q_2}c_{i2}, 2^{q_2}c_{i4}, \frac{\beta_i}{2}\right\}$. According to (34) and Lemma 1, the convergence time is calculated as,

$$t_s \leq t_{s,max} = \frac{1}{G_3\iota_1(1-q_1)} + \frac{1}{G_4\iota_1(q_2-1)}$$

where $\iota_1 \in (0,1)$. Moreover, when $t \to t_s$, it has,

$$\begin{aligned}
|z_{i1}| \leq& \sqrt{2\min\left\{G_3^{-\frac{1}{q_1}}\left(\frac{\Delta_{V_2}}{1-\iota_1}\right)^{\frac{1}{q_1}}, G_4^{-\frac{1}{q_2}}\left(\frac{\Delta_{V_2}}{1-\iota_1}\right)^{\frac{1}{q_2}}\right\}}\\
|z_{i2}| \leq& \sqrt{2\min\left\{G_3^{-\frac{1}{q_1}}\left(\frac{\Delta_{V_2}}{1-\iota_1}\right)^{\frac{1}{q_1}}, G_4^{-\frac{1}{q_2}}\left(\frac{\Delta_{V_2}}{1-\iota_1}\right)^{\frac{1}{q_2}}\right\}}\\
|\tilde{\theta}_i| \leq& \sqrt{2\bar{\gamma}\min\left\{G_3^{-\frac{1}{q_1}}\left(\frac{\Delta_{V_2}}{1-\iota_1}\right)^{\frac{1}{q_1}}, G_4^{-\frac{1}{q_2}}\left(\frac{\Delta_{V_2}}{1-\iota_1}\right)^{\frac{1}{q_2}}\right\}}
\end{aligned}$$

where $\bar{\gamma} = \max\{\gamma_{11}, \ldots, \gamma_{N1}\}$.

Moreover, it can be noticed that $|u_{ic}(t) - u_{io}(t)| < \vartheta_{i1}|u_{io}(t)| + \vartheta_{i2},\ \forall t \in \left[t_{k_i}^i, t_{k_{i+1}}^i\right)$. Based on the discussion in [16], the differentiability is ensured with respect to (32). Furthermore, we have,

$$\frac{d\,|E_i(t)|}{dt} = \frac{d}{dt}\left(E_i(t)E_i(t)\right)^{\frac{1}{2}} = \mathrm{sign}\left(E_i(t)\right)\dot{E}_i(t) \leq |\dot{u}_{ic}(t)|$$

Due to the bounded tracking errors, $\dot{u}_{ic}$ is bounded and $\dot{u}_{ic} \leq \mathscr{U}_i$ where $\mathscr{U}_i > 0$. Based on this, for the case when $\lim_{t\to t_{k_{i+1}}^i} E_i(t) = \vartheta_{i1}\left|u_{ic}\left(t_k^i\right)\right| + \vartheta_{i2} > 0$, then $t_{k_{i+1}}^i - t_{k_i}^i > \vartheta_{i2}/\mathscr{U}_i > 0$. A similar result can be obtained for the case when $\lim_{t\to t_{k_{i+1}}^i} E_i(t) = -\vartheta_{i1}\left|u_{ic}\left(t_k^i\right)\right| - \vartheta_{i2} < 0$. Consequently, the zeno behavior is avoided. ■

To achieve the multi lane fusion, an auxiliary variable λ_i is defined as $\lambda_i = \varpi_i e_{\sigma_i} + \dot{e}_{\sigma_i}$ where ϖ_i is a positive constant. The time derivative of λ_i satisfies,

$$\dot{\lambda}_i = \tau_i + \varpi_i(\phi_i - \dot{\delta}_i) - \ddot{\delta}_i \tag{35}$$

where $\varpi_i > 0$. Moreover, an event-triggered fixed-time control law for λ_i is designed. Similar to the previous deduction, the event-triggering mechanism is defined as,

$$\tau_{io}(t) = \tau_{ic}\left(t_{j_i}^i\right),\ \forall t \in \left[t_{j_i}^i, t_{j_{i+1}}^i\right) \tag{36}$$

$$t_{j_{i+1}}^i = \inf\left\{t > t_{j_i}^i \,||H_i(t)| \geq \vartheta_{i3}|\tau_{io}(t)| + \vartheta_{i4}\right\} \tag{37}$$

where $\tau_{io}(t)$ is an intermediate control variable, $0 < \vartheta_{i3} < 1$ and $\vartheta_{i4} > 0$. $t_{j_i}^i$ is the latest triggering time point of the ith vehicle. According to (36) and (37), it has,

$$|H_i(t)| = |\tau_{ic}(t) - \tau_{io}(t)| < \vartheta_{i3}|\tau_{io}(t)| + \vartheta_{i4}, \forall t \in \left[t_{j_i}^i, t_{j_{i+1}}^i\right)$$

Then $\tau_{ic}(t) = (1+\psi_{i3}(t)\vartheta_{i3})\,\tau_{io}(t) + \psi_{i4}(t)\vartheta_{i4}$ where $|\psi_{i3}(t)| \leq 1$ and $|\psi_{i4}(t)| \leq 1$. Consequently, it has,

$$\tau_{io}(t) = \frac{\tau_{ic}(t)}{1+\psi_{i3}(t)\vartheta_{i3}} - \frac{\psi_{i4}(t)\vartheta_{i4}}{1+\psi_{i3}(t)\vartheta_{i3}} \tag{38}$$

According to (35) and (38), the control law for λ_i is given as,

$$\tau_i = -\frac{\lambda_i\tau_{io}^2}{\sqrt{\lambda_i^2\tau_{io}^2+\varrho_i^2}} \tag{39}$$

$$\tau_{ic} = (1+\vartheta_{i3})\left[\mathscr{Q}_i\tanh\left(\frac{\lambda_i\mathscr{Q}_i}{\varsigma_{i2}}\right) + \bar{\vartheta}_{i2}\tanh\left(\frac{\lambda_i\bar{\vartheta}_{i2}}{\varsigma_{i2}}\right)\right] \tag{40}$$

where $\mathscr{Q}_i = c_{i5}\lambda_i^{2q_1-1} + c_{i6}\lambda_i^{2q_2-1} + \varpi_i(\phi_i - \dot{\delta}_i) - \ddot{\delta}_i$ and $\bar{\vartheta}_{i2} > \vartheta_{i4}/(1-\vartheta_{i3})$ with $c_{i5} > 0$ and $c_{i6} > 0$.

Theorem 3. *Considering the given 2-D platoon system in (1), the proposed event-triggered angle tracking controller (39) and (40) can ensure the fixed time convergence of the angle tracking error in (7).*

Proof: Here, we select the Lyapunov function as $V_3 = \sum_{i=1}^{N} \frac{1}{2}\lambda_i^2$. Then the derivation of V_3 holds,

$$\begin{aligned}\dot{V}_3 =& \sum_{i=1}^{N}\left[-\frac{\lambda_i^2\tau_{io}^2}{\sqrt{\lambda_i^2\tau_{io}^2+\varrho_i^2}}+\lambda_i\varpi_i(\phi_i-\dot{\delta}_i)-\lambda_i\ddot{\delta}_i\right]\\ \leq& \sum_{i=1}^{N}\left[\varrho_i-\frac{\lambda_i\tau_{ic}}{1+\vartheta_{i3}}+\left|\frac{\lambda_i\vartheta_{i4}}{1-\vartheta_{i3}}\right|+\lambda_i\varpi_i(\phi_i-\dot{\delta}_i)-\lambda_i\ddot{\delta}_i\right]\\ \leq& \sum_{i=1}^{N}\left(-c_{i5}\lambda_i^{2q_1}-c_{i6}\lambda_i^{2q_2}\right)+\Delta_{V_3}\\ \leq& -G_5V_3^{q_1}-G_6V_3^{q_2}+\Delta_{V_3}\end{aligned}$$

where $\Delta_{V_3} = \sum_{i=1}^{N}(\varrho_i + 0.557\varsigma_{i2})$, $G_5 = \min\{2^{q_1}c_{i5}\}$ and $G_6 = N^{1-q_2}\min\{2^{q_2}c_{i6}\}$. The convergence time satisfies,

$$t_\lambda \leq t_{\lambda,max} = \frac{1}{G_5\iota_2(1-q_1)} + \frac{1}{G_6\iota_2(q_2-1)}$$

where $\iota_2 \in (0,1)$. Moreover, when $t \to t_\lambda$ it has,

$$|\lambda_i| \leq \sqrt{2\min\left\{G_5^{-\frac{1}{q_1}}\left(\frac{\Delta_{V_3}}{1-\iota_2}\right)^{\frac{1}{q_1}}, G_6^{-\frac{1}{q_2}}\left(\frac{\Delta_{V_3}}{1-\iota_2}\right)^{\frac{1}{q_2}}\right\}}$$

As for the discussions about the zeno behavior, similar results can be found in the proof of Theorem 2. ■

Remark 9. *Although the distance constrained fusion control is discussed in [24], the communication burden is not considered. Indeed, the controller in [24] needs to be updated continuously with respect to the changing tracking errors. In the present paper, to reduce the communication burden, the event trigger-based fusion control strategy is studied and two separate event-triggered mechanisms independent of each other are introduced while making the vehicles track the desired vehicle distance and the velocity direction angle. Moreover, (28) and (36) show that u_{io} and τ_{io} will hold between each triggering interval. Therefore, the continuous communications for u_{ic} and τ_{ic} are not necessary and thus the computation burden for calculating u_{ic} and τ_{ic} is hence alleviated in (31) and (39).*

Remark 10. *Despite the fact that the proposed event-triggered fixed-time control technique includes several adjustable parameters, the major aim is to provide a quick and precise control input for the safety-critical vehicle platoon in light of restricted communication resources. Therefore, by retrospecting Lemma 1, large values of c_{ij}, $j = 1,\ldots,6$ can result in faster convergence of the tracking errors. As for ϑ_{i1}, ϑ_{i2}, ϑ_{i3}, ϑ_{i4} in (29) and (37), if ϑ_{i1} and ϑ_{i3} approach 0, then the relative threshold-based event triggering mechanism performs like the fixed threshold-based approach in [16] which needs more triggering events during the system stabilization process. According to the expressions of Δ_{V_2} and Δ_{V_3}, the parameters Υ_i and ϱ_i in (31) and (39) are suggested to be made small so as to achieve preciser error boundaries.*

Remark 11. *In (29) and (37), the triggering threshold is composed by a fixed term and a controller signal related part. According to [16], if there is a large control signal, it indicates that a large measurement error and a large triggering interval will be obtained and the communication and computation burdens are hence eased. When the control signal approaches to the equilibrium zero, the triggering threshold becomes smaller so as to provide a precise control process. Similar event triggering notions can be found in the time varying threshold method in [35], [36]. However, the threshold is independent from the system errors or the control signals. Therefore, the relative-threshold triggering mechanism can be regarded as the extension of these works.*

IV. Simulation

In this section, the simulation is executed in Matlab. All the results are given based on numerical simulation with the system model proposed in [24]. As is stated in [24], the unmodeled system dynamics and the external disturbances are expressed by s_i and T_{di} in (1). Moreover, the corresponding simulation results will be provided so as to validate the effectiveness of the proposed event-triggered multi-lane fusion control approach for straight and curved road case. Moreover, the comparison will be done between the given method and [24]. In the simulation, four vehicles are considered where Vehicle 0 is the virtual leader and Vehicle 1-3 are considered as the followers in sequence. The initial states of each vehicle are given in Tab.I. With reference to [24], the nonlinear term s_i and external disturbance T_{di} are selected as $s_i = -0.1176 - 0.0077616v_i - 0.00016v_i^2$ and $T_{di} = \sin(t + 0.25\pi i)$ $(i = 1,2,3)$. The desired distance d between each adjacent vehicle is set as $15m$. According to [24], the minimum collision avoidance gap is given as $\mathscr{D}_{col} = 8m$ and the maximum communication range holds that $\mathscr{D}_{con} = 21m$. The upper and lower bounds of S_{di} are selected as $S_d^+ = 10$ and $S_d^- = -10$ for case 1 and $S_d^+ = 5$ and $S_d^- = -5$ for case 2. According to [24], the acceleration of v_0 is chosen as,

$$a_0 = \begin{cases} 0.5t\ m/s^2, & 0s \leq t < 5s,\\ 2.5\ m/s^2, & 5s \leq t < 9s,\\ -4\ m/s^2, & 14s \leq t < 17s,\\ 0\ m/s^2, & \text{otherwise.}\end{cases}$$

The control parameters for each vehicle are given like **Signal Reconstruction:** $L_i = -3$, $\hat{\bar{v}}_i(0) = 1$, $\hat{\underline{v}}_i(0) = -1$ **Error Transformation:** $\Delta_{il\infty} = -1$, $\Delta_{iu\infty} = 1$, $\varsigma_{il} = 0.5$, $\varsigma_{iu} = 0.3$, $\bar{\Delta}_{il} = 0$, $\underline{\Delta}_{iu} = 0$ **Event-Triggered Controller:** $q_1 = 0.9$, $q_2 = 1.1$, $c_{i1} = 0.5$, $c_{i2} = 1.5$, $c_{i3} = 0.1$, $c_{i4} = 0.1$, $\gamma_i = 0.1$, $\kappa_{i1} = 0.5$, $\beta_i = 2$, $\vartheta_{i1} = 0.8$, $\vartheta_{i2} = 1$, $\bar{\vartheta}_{i1} = 5.2$, $\Upsilon_i = 1$, $\varsigma_{i1} = 1$, $\varpi_i = 1$, $c_{i5} = 0.2$, $c_{i6} = 0.5$, $\vartheta_{i3} = 0.8$, $\vartheta_{i4} = 1$, $\bar{\vartheta}_{i2} = 5.2$, $\varrho_i = 1$, $\varsigma_{i2} = 1$. The parameters of the method in [24] are selected by trials.

A. Unknown Input Reconstruction

As for the unknown input reconstruction, the corresponding interval estimations for v_i are firstly given in Fig.4. From

TABLE I
INITIAL STATES OF EACH VEHICLE

Parameter	Vehicle 0	Vehicle 1	Vehicle 2	Vehicle 3
$x_i(0)$	40	23	15	0
$y_i(0)$	0	5	-5	0
$v_i(0)$	0	0	0	0
$\sigma_i(0)$	0	0	0	0
$\phi_i(0)$	0	0	0	0

Fig.4, we find that once the initial conditions for the states satisfy $\underline{\hat{v}}_i(0) < v_i(0) < \hat{\bar{v}}_i(0)$, then $\underline{\hat{v}}_i(t) < v_i(t) < \hat{\bar{v}}_i(t)$ holds for $t \geq 0$ and $v_i(t)$ varies in the regions bounded by $\underline{\hat{v}}_i(t)$ and $\hat{\bar{v}}_i(t)$ which are marked in blue and red for case 1 and 2. Therefore, Theorem 1 is valid. Based on the interval estimation results, the time responses of the unknown input are depicted in Fig.5 which shows that the asymptotic convergent unknown input reconstruction is reached within $1s$. The reason behind the fast signal reconstruction is the algebraic calculation in (16). Moreover, Fig.5 also indicates that even though different selections for S_d^+ and S_d^- may be done, the reconstruction results can still be achieved swiftly and accurately.

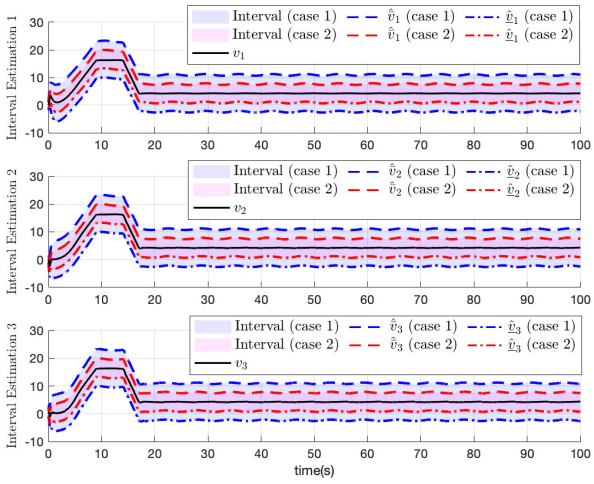

Fig. 4. The interval estimation for v_i.

B. Straight Road Case

In this section, Vehicle 0 is assumed to stay on a straight road. Therefore, the velocity angle σ_0 always holds that $\sigma_0 = 0$. As for time responses of the adaptive fuzzy fusion control regarding the distance keeping constraints, the corresponding results are given in Fig.6-9. In Fig.6-7, the trajectories alongside the X and Y axis for each vehicle are presented. The multi-lane vehicle fusion is presented in Fig.7. In Fig.8, the acceptable tracking error variance area is marked in red which is bounded by the predesigned constraints on the distance tracking error. Therefore, we can note that the distance tracking error e_i is always bounded by the predesigned distance tracking error constraints. However, the distance tracking error e_i in [24] is constrained by a fixed boundary set. In the present paper, the boundary set is selected

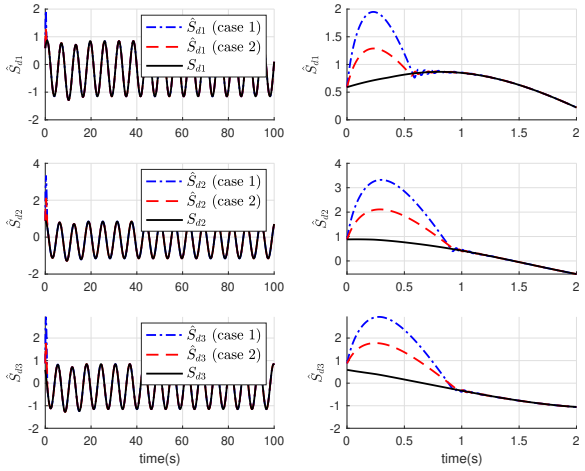

Fig. 5. The reconstruction results for S_{di}.

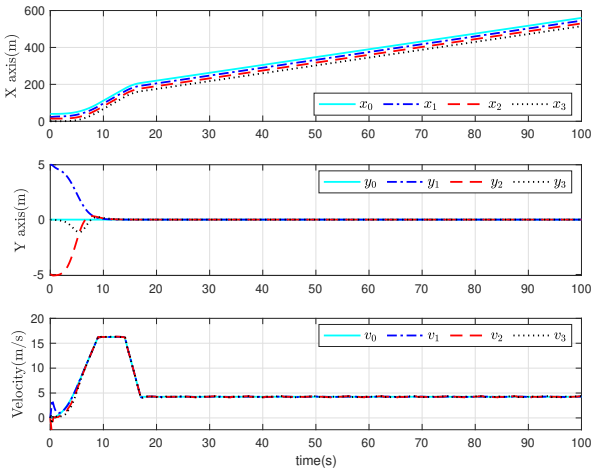

Fig. 6. The time responses for each vehicle's trajectory.

as a time-varying one, which is less conservative. Therefore, the proposed fusion control strategy in the present paper can be viewed as an extension of the work in [24]. Furthermore, due to the implement of the fixed time control strategy, faster time responses can be reached for distance tracking and angular tracking process. In Fig.8, the setting time for e_i is $2s$ by using the proposed method while for the approach in [24], it takes nearly $8s$ to stabilize e_i. The comprehensive distance and angular tracking processes in Fig.9 also demonstrate the swift control performance of the proposed strategy when compared to [24]. According to Fig.9, the multi-lane fusion processes are achieved within $10s$ and $25s$ for the given method and the strategy in [24], respectively. Therefore, the safety and reliability of the vehicle platoon are ensured. The control inputs for each vehicle are presented in Fig.10 and 12. The released intervals and instants are depicted in Fig.11 and 13. The detailed event triggering mechanism performance analysis is provided in Table.II.

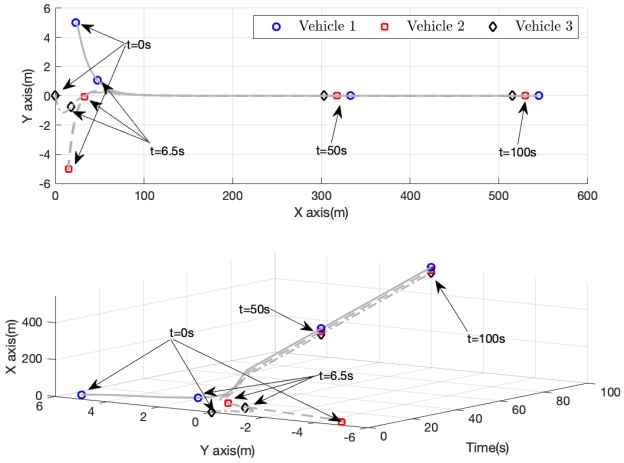

Fig. 7. The time response for the multi-lane vehicle fusion process.

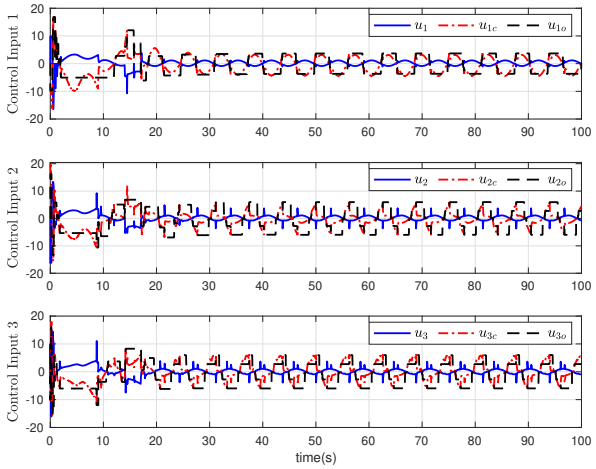

Fig. 10. The time responses for u_i, u_{ic}, and u_{io}.

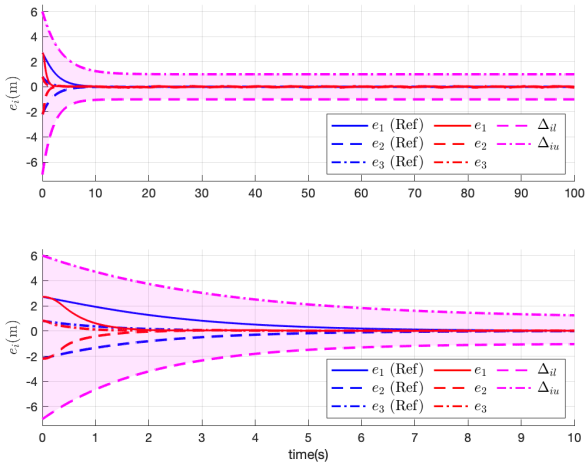

Fig. 8. Responses for the distance tracking error e_i in this paper and [24].

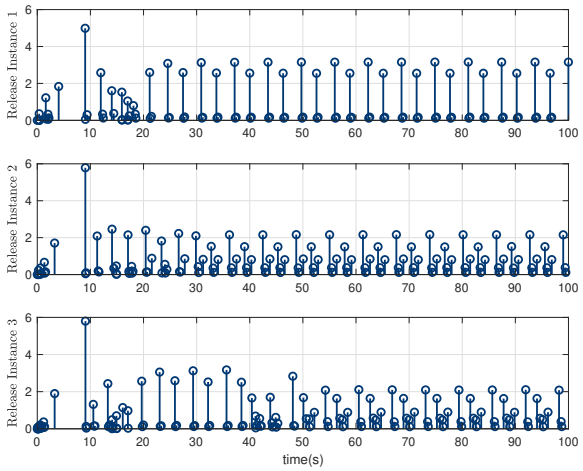

Fig. 11. The release instants and release interval for u_{io}.

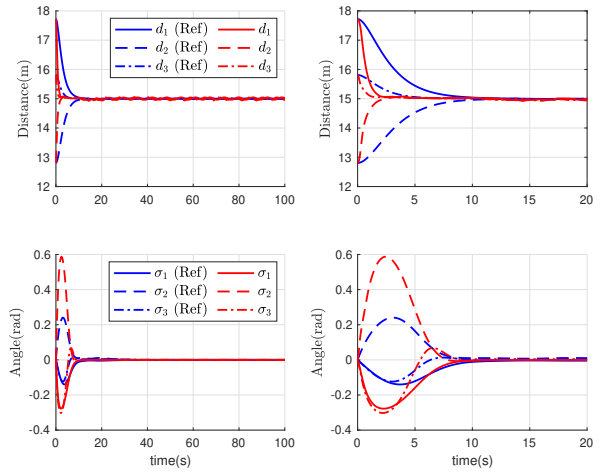

Fig. 9. Responses for the distance and velocity angle in this paper and [24].

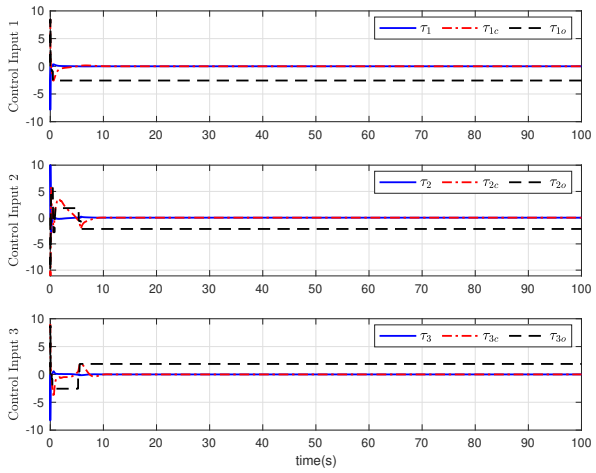

Fig. 12. The time responses for τ_i, τ_{ic}, and τ_{io}.

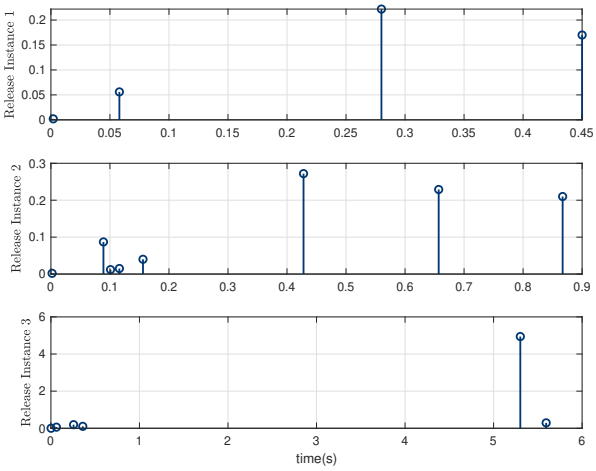

Fig. 13. The release instants and release interval for τ_{io}.

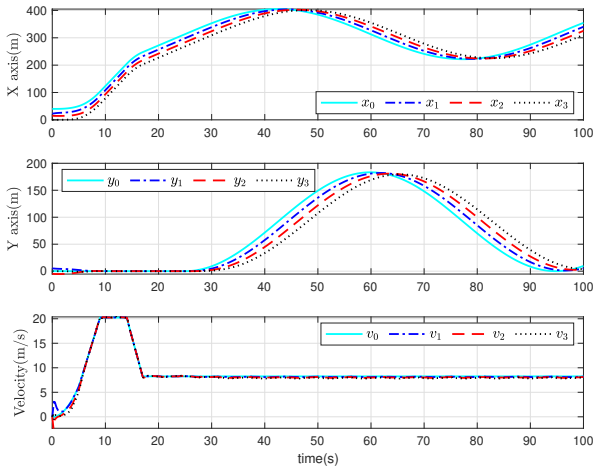

Fig. 14. The time responses for each vehicle's trajectory.

TABLE II
INFORMATION FOR THE RELEASED INTERVALS AND INSTANTS

Index (u_{io})	Vehicle 1	Vehicle 2	Vehicle 3
Number of triggers	105	133	140
Average Period	$0.952s$	$0.751s$	$0.714s$
Maximum Interval	$4.988s$	$5.786s$	$5.799s$
Index (τ_{io})	Vehicle 1	Vehicle 2	Vehicle 3
Number of triggers	4	8	6
Average Period	$25s$	12.5	$16.667s$
Maximum Interval	$0.222s$	$0.272s$	$4.942s$

C. Curved Road Case

In this section, the curved road is considered and the velocity angle $\sigma_0(t)$ is assumed to satisfy that,

$$\begin{cases} \sigma_0 = 0\ rad, \text{ and } \dot{\sigma}_0 = 0\ rad/s & 0s \le t < 25s, \\ \dot{\sigma}_0 = 0.09\ rad/s, & \text{otherwise.} \end{cases}$$

The the acceleration of v_0 is chosen as,

$$a_0 = \begin{cases} 0.5t\ m/s^2, & 0s \le t < 5s, \\ 3.5\ m/s^2, & 5s \le t < 9s, \\ -4\ m/s^2, & 14s \le t < 17s, \\ 0\ m/s^2, & \text{otherwise.} \end{cases}$$

Moreover, c_{i5}, c_{i6} and ϖ_i are selected as $c_{i5} = 0.5$, $c_{i6} = 1$ and $\varpi_i = 5$ in this case. The time responses of the systems with respect to the given method are depicted in Fig.14-17. The 2-D and 3-D lanes merging processes can be found in Fig.14-15 while the corresponding positions with respect to some certain timepoints are marked. In Fig.16, the responses for the distance tracking error e_i are provided. From Fig.16, it takes $2s$ to realize the distance keeping under the given controller. Moreover, it notes that the possible singularity problem is avoided in this paper because of the implement of atan2 function. In Fig.17, once the velocity angle σ_i crosses π, the value of σ_i will be mapped into the negative quadrants. The multi-lane fusion is achieved within $10s$. The control inputs are presented in Fig.18 and 20. The released intervals and instants

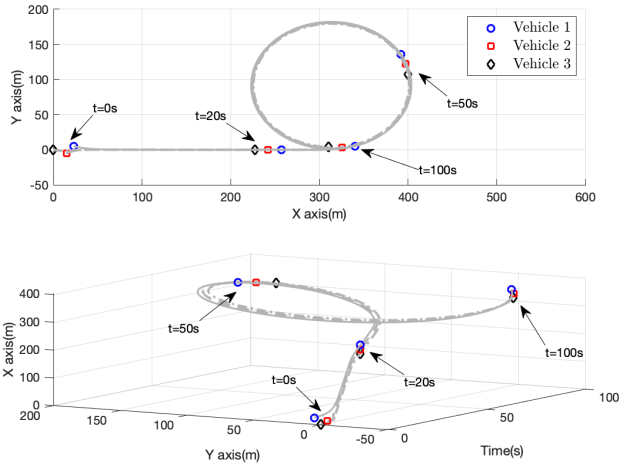

Fig. 15. The time response for the multi-lane vehicle fusion process.

are depicted in Fig.19 and 21. The detailed event triggering mechanism performance analysis is provided in Table.III.

TABLE III
INFORMATION FOR THE RELEASED INTERVALS AND INSTANTS

Index (u_{io})	Vehicle 1	Vehicle 2	Vehicle 3
Number of triggers	108	135	139
Average Period	$0.926s$	$0.74s$	$0.72s$
Maximum Interval	$5.133s$	$6.339s$	$5.112s$
Index (τ_{io})	Vehicle 1	Vehicle 2	Vehicle 3
Number of triggers	14	17	13
Average Period	$7.14s$	$5.88s$	$7.69s$
Maximum Interval	$1.336s$	$3.285s$	$4.375s$

V. CONCLUSION

In this paper, the multi-lane fusion problem for a 2-D vehicle platoon system is investigated and an adaptive fuzzy fusion control strategy is proposed. As for compensating the

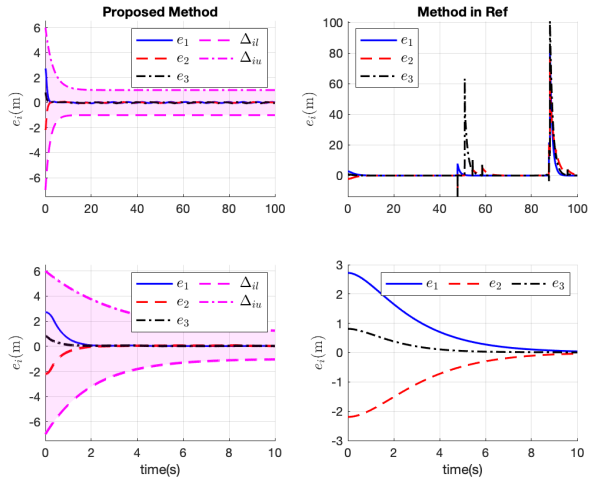

Fig. 16. Responses for the distance tracking error e_i in this paper and [24].

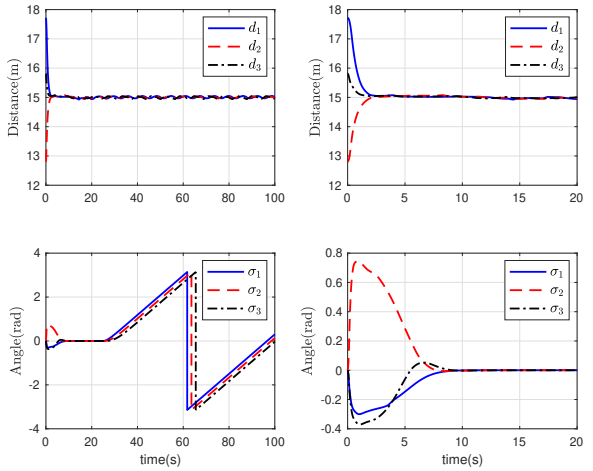

Fig. 17. Responses for the distance and velocity angle in this paper.

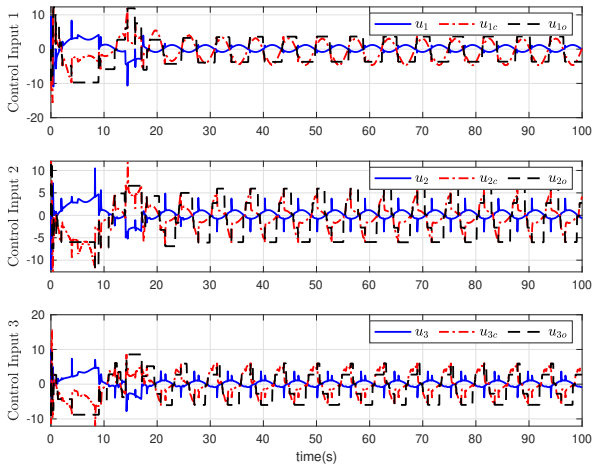

Fig. 18. The time responses for u_i, u_{ic}, and u_{io}.

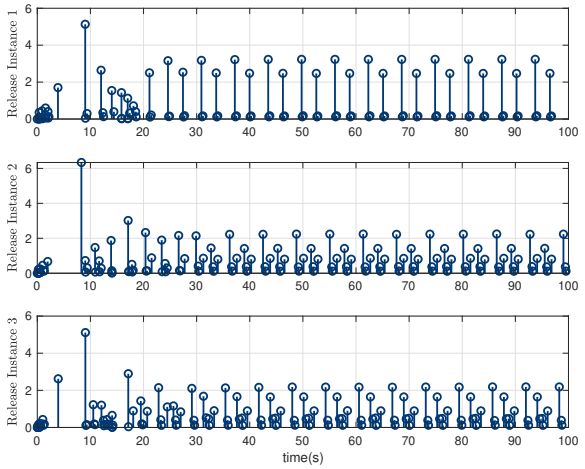

Fig. 19. The release instants and release interval for u_{io}.

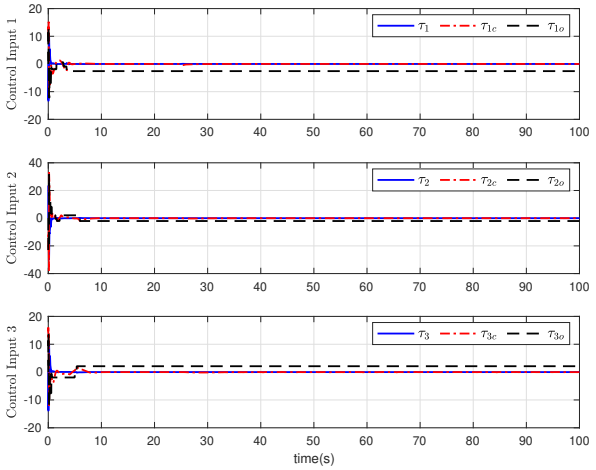

Fig. 20. The time responses for τ_i, τ_{ic}, and τ_{io}.

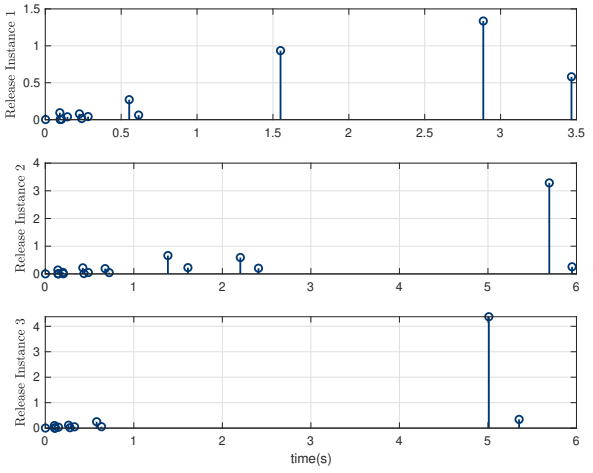

Fig. 21. The release instants and release interval for τ_{io}.

impacts caused by the unknown system dynamics and the external disturbance, an algebraic calculation-based unknown input reconstruction method is developed on the basis of the interval estimation results. To avoid the collision and lose of effective communication, the distance keeping rule is considered and a barrier function-based distance constrained control method is hence presented. In addition, the errors between the ideal virtual controller and the one generated by command filter are offset by the adaptive fuzzy logic system. Moreover, because of the limited communication resources, the event trigger mechanism using the relative threshold technique is imported to the adaptive fuzzy fixed-time controller. The future working direction may involve input saturations and the time delays in the 2-D vehicle platoon system.

REFERENCES

[1] Q. Chen, Y. Zhou, S. Ahn, J. Xia, S. Li, and S. Li, "Robustly string stable longitudinal control for vehicle platoons under communication failures: A generalized extended state observer-based control approach," *IEEE Transactions on Intelligent Vehicles*, pp. 1–1, 2022.

[2] Z. Xu and X. Jiao, "Robust control of connected cruise vehicle platoon with uncertain human driving reaction time," *IEEE Transactions on Intelligent Vehicles*, pp. 1–1, 2021.

[3] A. Khalifa, O. Kermorgant, S. Dominguez, and P. Martinet, "Platooning of car-like vehicles in urban environments: Longitudinal control considering actuator dynamics, time delays, and limited communication capabilities," *IEEE Transactions on Control Systems Technology*, vol. 29, no. 6, pp. 2670–2677, 2021.

[4] S. D. Kumaravel, A. Malikopoulos, and R. Ayyagari, "Optimal coordination of platoons of connected and automated vehicles at signal-free intersections," *IEEE Transactions on Intelligent Vehicles*, pp. 1–1, 2021.

[5] Xu, R. and Guo, Y. and Han, X. and Xia, X. and Xiang, H. and Ma, J., "OpenCDA: An Open Cooperative Driving Automation Framework Integrated with Co-Simulation," in *2021 IEEE International Intelligent Transportation Systems Conference (ITSC)*, Conference Proceedings, pp. 1155–1162.

[6] Han, Xu and Xu, Runsheng and Xia, Xin and Sathyan, Anoop and Guo, Yi and Bujanović, Pavle and Leslie, Edward and Goli, Mohammad and Ma, Jiaqi, "Strategic and Tactical Decision-Making for Cooperative Vehicle Platooning with Organized Behavior on Multi-Lane Highways," *SSRN*, pp. 1–38.

[7] C. K. Verginis, C. P. Bechlioulis, D. V. Dimarogonas, and K. J. Kyriakopoulos, "Robust distributed control protocols for large vehicular platoons with prescribed transient and steady-state performance," *IEEE Transactions on Control Systems Technology*, vol. 26, no. 1, pp. 299–304, 2018.

[8] Y. Liu, D. Yao, H. Li, and R. Lu, "Distributed cooperative compound tracking control for a platoon of vehicles with adaptive nn," *IEEE Transactions on Cybernetics*, pp. 1–10, 2021.

[9] D. Li, H. Han, and J. Qiao, "Observer-based adaptive fuzzy control for nonlinear state-constrained systems without involving feasibility conditions," *IEEE Transactions on Cybernetics*, pp. 1–10, 2021.

[10] X. G. Guo, W. D. Xu, J. L. Wang, J. H. Park, and H. C. Yan, "Blf-based neuroadaptive fault-tolerant control for nonlinear vehicular platoon with time-varying fault directions and distance restrictions," *IEEE Transactions on Intelligent Transportation Systems*, pp. 1–11, 2021.

[11] O. Elhaki and K. Shojaei, "Observer-based neural adaptive control of a platoon of autonomous tractor-trailer vehicles with uncertain dynamics," *IET Control Theory and Applications*, vol. 14, no. 14, pp. 1898–1911, 2020.

[12] S. L. Dai, S. D. He, H. Lin, and C. Wang, "Platoon formation control with prescribed performance guarantees for usvs," *IEEE Transactions on Industrial Electronics*, vol. 65, no. 5, pp. 4237–4246, 2018.

[13] O. Elhaki and K. Shojaei, "Robust prescribed performance-based control of autonomous tractor-trailers convoy with limited communication range," *International Journal of Systems Science*, vol. 52, no. 3, pp. 555–582, 2021.

[14] D. Li and G. Guo, "Prescribed performance concurrent control of connected vehicles with nonlinear third-order dynamics," *IEEE Transactions on Vehicular Technology*, vol. 69, no. 12, pp. 14 793–14 802, 2020.

[15] J. Wang, W. C. Wong, X. Luo, X. Li, and X. Guan, "Connectivity-maintained and specified-time vehicle platoon control systems with disturbance observer," *International Journal of Robust and Nonlinear Control*, vol. 31, no. 16, pp. 7844–7861, 2021.

[16] L. Xing, C. Wen, Z. Liu, H. Su, and J. Cai, "Event-triggered adaptive control for a class of uncertain nonlinear systems," *IEEE Transactions on Automatic Control*, vol. 62, no. 4, pp. 2071–2076, 2017.

[17] L. Cao, H. Li, N. Wang, and Q. Zhou, "Observer-based event-triggered adaptive decentralized fuzzy control for nonlinear large-scale systems," *IEEE Transactions on Fuzzy Systems*, vol. 27, no. 6, pp. 1201–1214, 2019.

[18] Y. Deng and X. Zhang, "Event-triggered composite adaptive fuzzy output-feedback control for path following of autonomous surface vessels," *IEEE Transactions on Fuzzy Systems*, vol. 29, no. 9, pp. 2701–2713, 2021.

[19] T. Jia, Y. Pan, H. Liang, and H. K. Lam, "Event-based adaptive fixed-time fuzzy control for active vehicle suspension systems with time-varying displacement constraint," *IEEE Transactions on Fuzzy Systems*, pp. 1–1, 2021.

[20] Y. Salmanpour, M. M. Arefi, A. Khayatian, and O. Kaynak, "Event-triggered fuzzy adaptive leader-following tracking control of non-affine multi-agent systems with finite-time output constraint and input saturation," *IEEE Transactions on Fuzzy Systems*, pp. 1–1, 2021.

[21] L. Wang and J. Dong, "Adaptive fuzzy consensus tracking control for uncertain fractional-order multi-agent systems with event-triggered input," *IEEE Transactions on Fuzzy Systems*, pp. 1–1, 2020.

[22] H. Zhang, J. Liu, Z. Wang, H. Yan, and C. Zhang, "Distributed adaptive event-triggered control and stability analysis for vehicular platoon," *IEEE Transactions on Intelligent Transportation Systems*, vol. 22, no. 3, pp. 1627–1638, 2021.

[23] H. Zhang, J. Liu, Z. Wang, C. Huang, and H. Yan, "Adaptive switched control for connected vehicle platoon with unknown input delays," *IEEE Transactions on Cybernetics*, pp. 1–11, 2021.

[24] X. G. Guo, W. D. Xu, J. L. Wang, and J. H. Park, "Distributed neuroadaptive fault-tolerant sliding-mode control for 2-d plane vehicular platoon systems with spacing constraints and unknown direction faults," *Automatica*, vol. 129, p. 109675, 2021.

[25] G. J. L. Naus, R. P. A. Vugts, J. Ploeg, M. J. G. v. d. Molengraft, and M. Steinbuch, "String-stable cacc design and experimental validation: A frequency-domain approach," *IEEE Transactions on Vehicular Technology*, vol. 59, no. 9, pp. 4268–4279, 2010.

[26] X. K. He, E. Hashemi, and K. H. Johansson, "Distributed control under compromised measurements: Resilient estimation, attack detection, and vehicle platooning," *Automatica*, vol. 134, p. 109953, 2021.

[27] A. Liu, T. Li, Y. Gu, and H. H. Dai, "Cooperative extended state observer based control of vehicle platoons with arbitrarily small time headway," *Automatica*, vol. 129, p. 109678, 2021.

[28] J. Liu, Y. Zhang, Y. Yu, and C. Sun, "Fixed-time event-triggered consensus for nonlinear multiagent systems without continuous communications," *IEEE Transactions on Systems, Man, and Cybernetics: Systems*, vol. 49, no. 11, pp. 2221–2229, 2019.

[29] Y. Liu and Q. Zhu, "Event-triggered adaptive neural network control for stochastic nonlinear systems with state constraints and time-varying delays," *IEEE Transactions on Neural Networks and Learning Systems*, pp. 1–13, 2021.

[30] M. Chen, H. Wang, and X. Liu, "Adaptive fuzzy practical fixed-time tracking control of nonlinear systems," *IEEE Transactions on Fuzzy Systems*, vol. 29, no. 3, pp. 664–673, 2021.

[31] Y. Liu and Q. Zhu, "Adaptive fuzzy finite-time control for nonstrict-feedback nonlinear systems," *IEEE Transactions on Cybernetics*, pp. 1–10, 2021.

[32] A. Levant, "Higher-order sliding modes, differentiation and output-feedback control," *International Journal of Control*, vol. 76, no. 9-10, pp. 924–941, 2003.

[33] L. Liu, T. Gao, Y. J. Liu, S. Tong, C. L. P. Chen, and L. Ma, "Time-varying iblfs-based adaptive control of uncertain nonlinear systems with full state constraints," *Automatica*, vol. 129, p. 109595, 2021.

[34] J. Yu, L. Zhao, H. Yu, and C. Lin, "Barrier lyapunov functions-based command filtered output feedback control for full-state constrained nonlinear systems," *Automatica*, vol. 105, pp. 71–79, 2019.

[35] X. Fan and Z. Wang, "Event-triggered integral sliding mode control for linear systems with disturbance," *Systems & Control Letters*, vol. 138, p. 104669, 2020.

[36] Z. Echreshavi, M. Farbood, and M. Shasadeghi, "Fuzzy event-triggered integral sliding mode control of nonlinear continuous-time systems," *IEEE Transactions on Fuzzy Systems*, pp. 1–1, 2021.